OPEN

Intestinal Microbial Variation May Predict Early Acute Rejection after Liver Transplantation in Rats

Zhigang Ren,[1,2] Jianwen Jiang,[1,2] Haifeng Lu,[3] Xinhua Chen,[1,2] Yong He,[1,2] Hua Zhang,[3] Haiyang Xie,[1,2] Weilin Wang,[1,2] Shusen Zheng,[1,2,5] and Lin Zhou[1,2,4]

Background. Acute rejection (AR) remains a life-threatening complication after orthotopic liver transplantation (OLT) and there are few available diagnostic biomarkers clinically for AR. This study aims to identify intestinal microbial profile and explore potential application of microbial profile as a biomarker for AR after OLT.
Methods. The OLT models in rats were established. Hepatic graft histology, ultrastructure, function, and intestinal barrier function were tested. Ileocecal contents were collected for intestinal microbial analysis.
Results. Hepatic graft suffered from the ischemia-reperfusion (I/R) injury on day 1, initial AR on day 3, and severe AR on day 7 after OLT. Real-time quantitative polymerase chain reaction results showed that genus *Faecalibacterium prausnitzii* and *Lactobacillus* were decreased, whereas *Clostridium bolteae* was increased during AR. Notably, cluster analysis of denaturing gradient gel electrophoresis (DGGE) profiles showed the 7AR and 3AR groups clustered together with 73.4% similarity, suggesting that intestinal microbiota was more sensitive than hepatic function in responding to AR. Microbial diversity and species richness were decreased during AR. Phylogenetic tree analysis showed that most of the decreased key bacteria belonged to phylum *Firmicutes*, whereas increased key bacteria belonged to phylum *Bacteroidetes*. Moreover, intestinal microvilli loss and tight junction damage were noted, and intestinal barrier dysfunction during AR presented a decrease of fecal secretory immunoglobulin A (sIgA) and increase of blood bacteremia, endotoxin, and tumor necrosis factor-α.
Conclusion. We dynamically detail intestinal microbial characterization and find a high sensitivity of microbial change during AR after OLT, suggesting that intestinal microbial variation may predict AR in early phase and become an assistant therapeutic target to improve rejection after OLT.

Key Words: Liver transplantation, Acute rejection, Intestinal microbiota, Microbiota-liver axis

(*Transplantation* 2014;98: 844–852)

Nowadays, orthotopic liver transplantation (OLT) has been a routine treatment of irreversible acute and chronic liver diseases (*1, 2*). In latest 30 years, the successful rates of OLT have increased steadily, and the unadjusted 1-year survival has reached 88.2% (*3*). In 2012 alone, 6,256 adult liver transplants were performed, and more than 65,000 people were living with a transplanted liver in the United States (*4*). However, acute rejection (AR) after OLT is still a life-threatening complication (*5*), and there are few available diagnostic biomarkers clinically for AR, thus, the identification of the rapid and noninvasive diagnostic tools is critically needed.

Currently, intestinal microbiota has been recognized as the most important microecosystem and a major metabolic "organ" that keeps a symbiotic relationship with the body (*6–8*). The human gut accommodates approximately

The authors declare no funding or conflicts of interest.
This work was supported by the National Basic Research Program (973 Program) in China (2013CB531403, 2013CB531401), National S&T Major Project of China (2012ZX10002-017), Natural Science Foundation of China (81372425), NSFC for Innovative Research Group of China (81121002), and Natural Science Foundation of Zhejiang Province (LY13H030002).
[1] Key Laboratory of Combined Multi-organ Transplantation, Ministry of Public Health, First Affiliated Hospital, School of Medicine, Zhejiang University, Hangzhou, China.
[2] Department of Hepatobiliary and Pancreatic Surgery, First Affiliated Hospital, School of Medicine, Zhejiang University, Hangzhou, China.
[3] State Key Laboratory for Diagnosis and Treatment of Infectious Disease, First Affiliated Hospital, School of Medicine, Zhejiang University, Hangzhou, China.
[4] Correspondence to: Lin Zhou, M.D., Ph.D., First Affiliated Hospital, School of Medicine, Zhejiang University, #79 Qingchun Road, Hangzhou, China.
[5] Correspondence to: Shusen Zheng, M.D., Ph.D., First Affiliated Hospital, School of Medicine, Zhejiang University, #79 Qingchun Road, Hangzhou, China.
E-mail: shusenzheng@zju.edu.cn. E-mail: zhoulin99@zju.edu.cn

Supplemental digital content (SDC) is available for this article. Direct URL citations appear in the printed text, and links to the digital files are provided in the HTML text of this article on the journal's website (www.transplantjournal.com).
Received 18 February 2014. Revision requested 16 March 2014.
Accepted 29 May 2014.
Z.R. and J.J. contributed equally to this study.
L.Z. and S.Z. conceived and designed the experiments. Z.R., J.J., H.L., X.C., Y.H., and H.Z. performed the experiments. Z.R., J.J., and H.L. analyzed the data. W.W., S.Z., and L.Z. contributed reagents, materials, and analysis tools. Z.R. wrote the article.

ISSN: 0041-1337/14/9808-844
DOI: 10.1097/TP.0000000000000334

400 different species of bacteria and comprises 10^{13} to 10^{14} microorganisms whose total genome contains more than 100 times of human beings genome (*6, 9*). Although intestinal microbiota plays crucial roles on various beneficial functions, including digestion of complex plant polysaccharides, maturity of initial immune system, and resistance to the invasion of enteric pathogens (*10, 11*), it has been associated with a spectrum of human diseases, such as inflammatory bowel diseases (*12*), liver cirrhosis (*13*), and hepatocellular carcinoma (*14*). Moreover, recent reports have indicated that intestinal transplantation results in colonic flora dysbiosis (*15, 16*), and AR after liver transplantation induces fecal microbial changes in rats (*17*).

The intimate anatomic and functional relationship between the intestine and the liver closely links both in health and disease. Hepatic injury or diseases, such as hepatic I/R injury (*18, 19*), alcoholic steatohepatitis (*20*), and liver cirrhosis (*13*), always follow alterations in intestinal

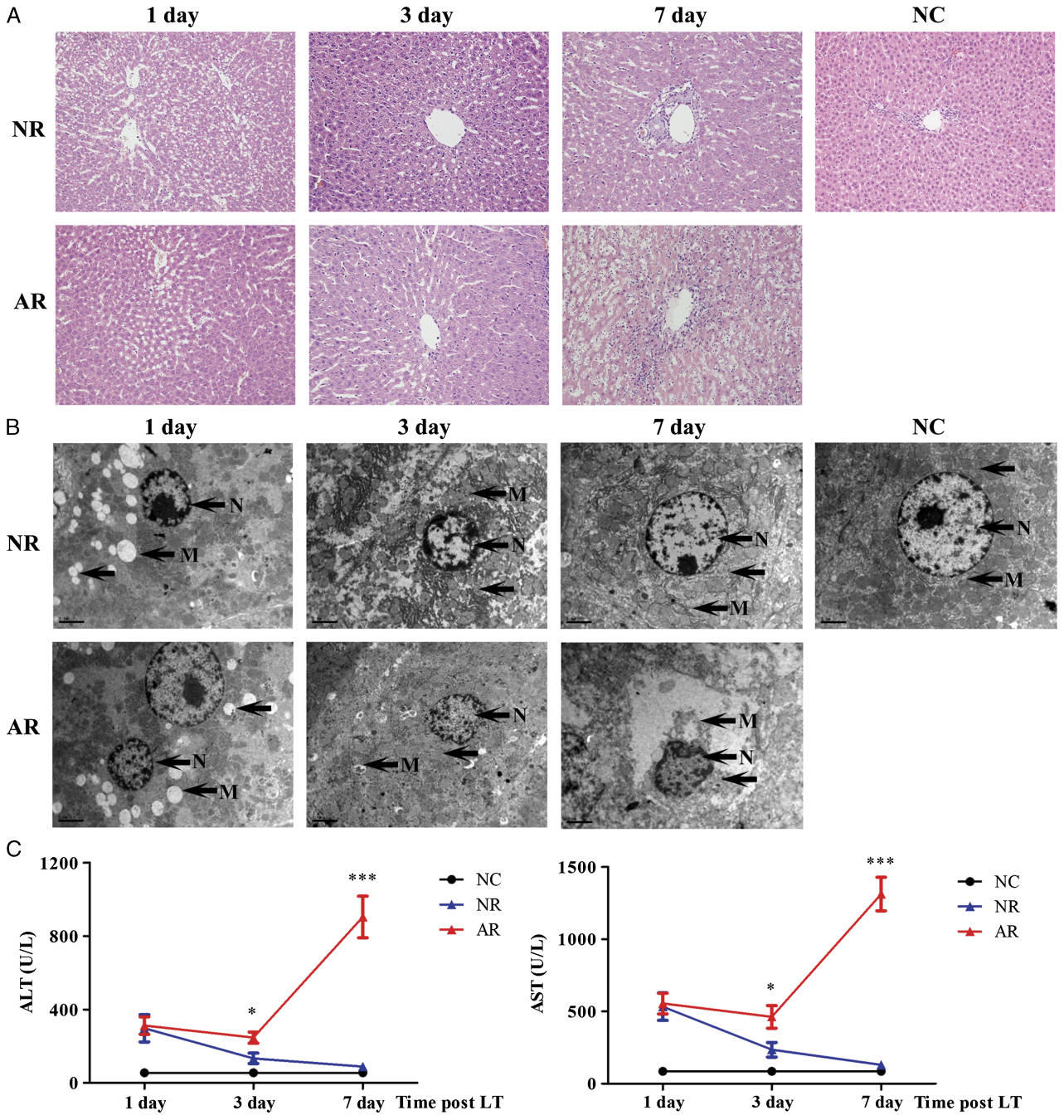

FIGURE 1. Dynamic alterations of hepatic graft structure and function during AR after OLT. A, representative hepatic graft histopathology stained with H&E (, 200×). B, representative hepatocytes ultrastructure observed by TEM. C, changes of plasma levels of ALT and AST at different time points after OLT. H&E, hematoxylin-eosin; TEM, transmission electron microscopy; AR, acute rejection; OLT, orthotopic liver transplantation; N, cell nucleus; M, mitochondria.

permeability and microbial composition. Meanwhile, under disease condition, intestinal microbial imbalance can aggravate liver injury and chronic inflammatory disease (*20*), ultimately promoting hepatocellular carcinoma (*14*). Nevertheless, it remains unclear that intestinal microbial dysbiosis is a cause or a consequence of hepatic injury or diseases.

In this study, we established the AR model of OLT and dynamically observed the relationship between microbial imbalance and liver rejection to identify intestinal microbial profile and explore potential application of microbial profile as a biomarker for AR after OLT.

RESULTS

Dynamic Alterations of Hepatic Graft Structure and Function After OLT

For the AR group, hepatic graft suffered from the I/R injury on day 1, initial AR on day 3, and severe AR on day 7 after OLT, thus the graft structure and function presented a dynamic alteration (Fig. 1).

Under light microscope (Fig. 1A), the liver in the normal control (NC) group showed a normal structure with well-arranged hepatocyte cords. Both the nonrejection (NR) and AR groups presented a disarray of hepatocyte cords, hepatocyte vacuolization, and widened sinusoids on day 1 after OLT. Hepatic graft injury was attenuated in the NR group, but aggravated in the AR group on days 3 and 7. Especially on day 7, lots of hepatocytes necrosis was noted in the AR group.

Hepatic graft ultrastructure presented a similar change (Fig. 1B). On day 1, lots of lipid droplets and mild karyopyknosis appeared in hepatocytes in both NR and AR groups. On days 3 and 7, hepatocytes morphology gradually restored near normal level in the NR group, but the obvious karyopyknosis and organelle breakdown were observed in the AR group.

Compared with NC group, plasma alanine aminotransferase (ALT) and aspartate aminotransferase (AST) were significantly increased in both NR and AR groups on day 1 ($P<0.01$ and 0.001, respectively). On day 3, both ALT and AST were decreased in the NR versus AR groups. On day 7, plasma ALT and AST decreased near normal level in the NR group, but obviously increased in the AR group (Fig. 1C).

Dynamic Quantification of Fecal Microbiota During AR After OLT

The dynamic comparisons of dominant bacterial groups by real-time quantitative polymerase chain reaction (RT-qPCR) between the NR and AR groups were shown in Figure 2. *Faecalibacterium prausnitzii* was significantly reduced in the AR versus NR group on day 7 ($P<0.01$). *Lactobacillus* was also decreased in the AR group ($P<0.05$). Contrastingly, *Clostridium bolteae* was obviously enriched in the AR group compared with NR group on day 7 ($P<0.01$). Other bacteria groups did not show any statistical difference among different groups.

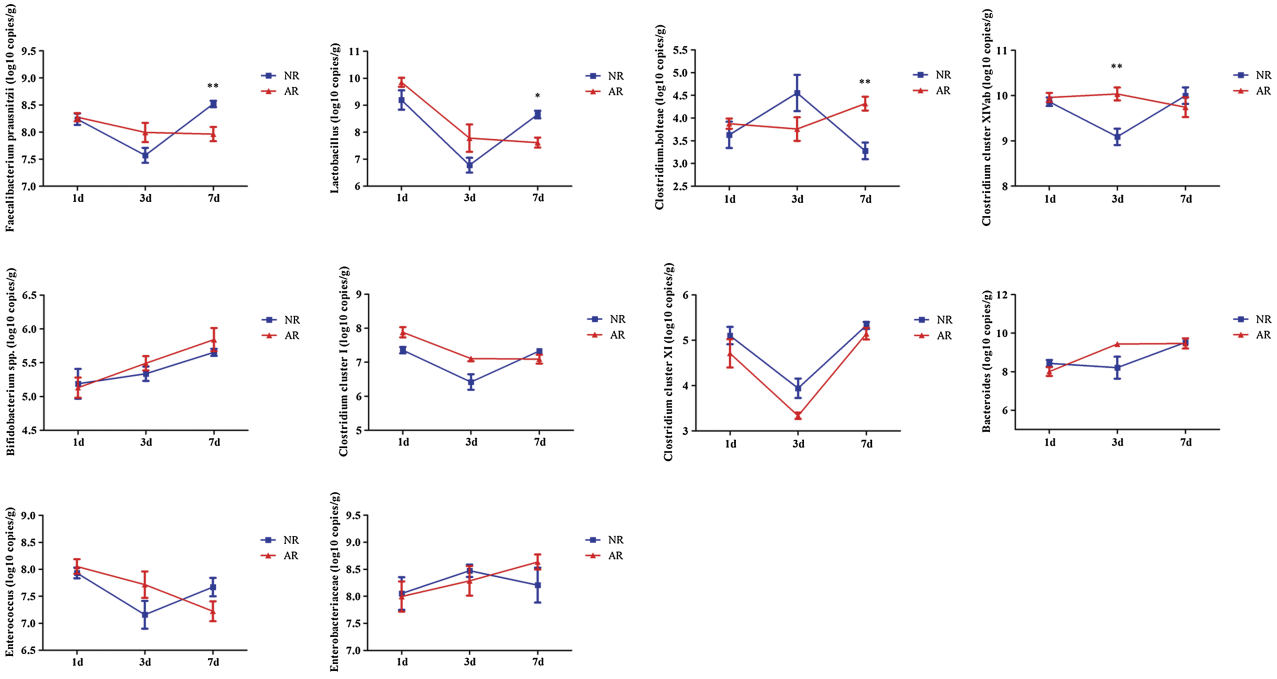

FIGURE 2. Dynamic quantification of fecal microbiota during AR after OLT. On the level of bacterial genus, dominant bacterial populations were analyzed by RT-qPCR between the NR and AR groups at different time points after OLT. The dominant bacteria mainly included *Faecalibacterium prausnitzii*, Clostridium clusters I, Clostridium clusters XI, Clostridium cluster XIVab, *Clostridium bolteae*, Bacteroides, *Bifidobacterium* species, Lactobacillus, Enterococcus and Enterobacteriaceae. Statistical differences were analyzed by *t* test between NR and AR groups. Log10 copies/g: log10 no. of 16S rDNA gene copies per gram feces (wet weight). *$P<0.05$, **$P<0.01$. AR, acute rejection; OLT, orthotopic liver transplantation; NR, nonrejection; RT-qPCR, real-time quantitative polymerase chain reaction;

Cluster Analysis and Diversity Analysis of DGGE Profiles

DGGE profiles of ileocecal microbiota presented changes of microbial composition. To analyze DGGE profiles characteristics, we utilized Dice coefficient and unweighted pair-group method with arithmetic means as a cluster method to indicate band pattern similarity (Fig. 3A). These profiles formed three primary clusters. The left cluster consisted of samples from NC, 7NR, and 3NR groups, in which the total similarity was 80.4%. The middle cluster contained samples of 1AR and 1NR groups with 75.1% total similarity. The right cluster accommodated 7AR and 3AR groups with 73.4% similarity. Meanwhile, the similarity among lanes from each group ranged from 78.7% to 95.2%, suggesting a uniqueness and stability of samples from each group.

Moreover, cluster characteristics of DGGE profiles were confirmed by multidimensional scaling (Fig. 3B) and principal components analysis (Fig. 3C). The distance between two data points represents the diversity of microbial compositions between two samples. Microbial structures of samples from the NC, 7NR, and 3NR groups, the 1AR and 1NR groups, as well as the 7AR and 3AR groups were, respectively, clustered together and showed a separation from each other by multidimensional scaling (Dim 1, Dim 2, and Dim 3) and principal components analysis axis X-Y-Z (19.2%, 16.4%, and 10.6%, respectively).

We analyzed microbial diversity using Past software (Fig. 3D). Compared to NC group, Shannon's diversity index was decreased in the NR ($P<0.05$) and AR groups ($P<0.001$) on day 1 and reduced in the AR group ($P<0.05$) on day 7, although Shannon's evenness index did not show any obvious difference among different groups. Meanwhile, compared with NC group, species richness was reduced in the NR ($P<0.05$) and AR groups ($P<0.001$) on day 1, as well as the AR group on day 7 ($P<0.05$).

Phylogenetic Tree Analysis of Sequences in DGGE Profiles

In the 56 PCR-DGGE bands analyzed in the study, 42 band classes were identified, in which 28 had little variation in band intensity among different groups. Compared to the

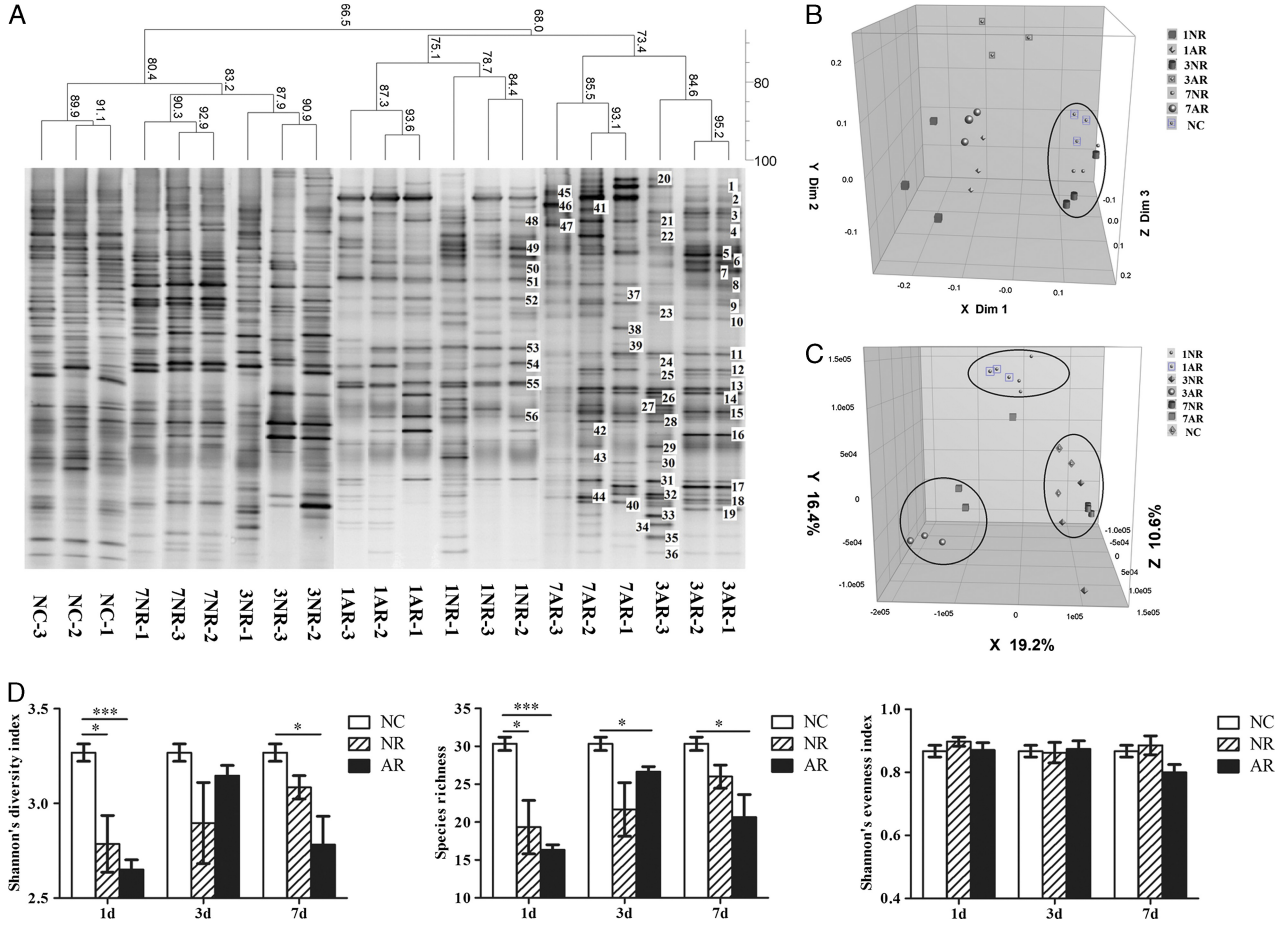

FIGURE 3. Cluster analysis and diversity analysis of DGGE profiles with universal primers V3 using Dice's coefficient and unweighted pair-group method with arithmetic means. A, cluster analysis of DGGE profiles from the different groups. Metric scale denotes the degree of similarity. Band numbers (corresponding to Fig. 4E band classes) indicated the position of bands excised for sequence. B, MDS analysis based on DGGE fingerprinting. The plot is an optimized three-dimensional representation of the similarity matrix obtained from BioNumerics software. C, PCA based on DGGE fingerprinting. It reorients the plot to maximize the variation among lanes along the first three principal components (the contributions 19.2, 16.4, and 10.6, respectively). (D) Intestinal microbial diversity analysis including Shannon's diversity index, species richness, and Shannon's evenness index among the different groups. *$P<0.05$, ***$P<0.001$. MDS, multidimensional scaling; PCA, principal components analysis.

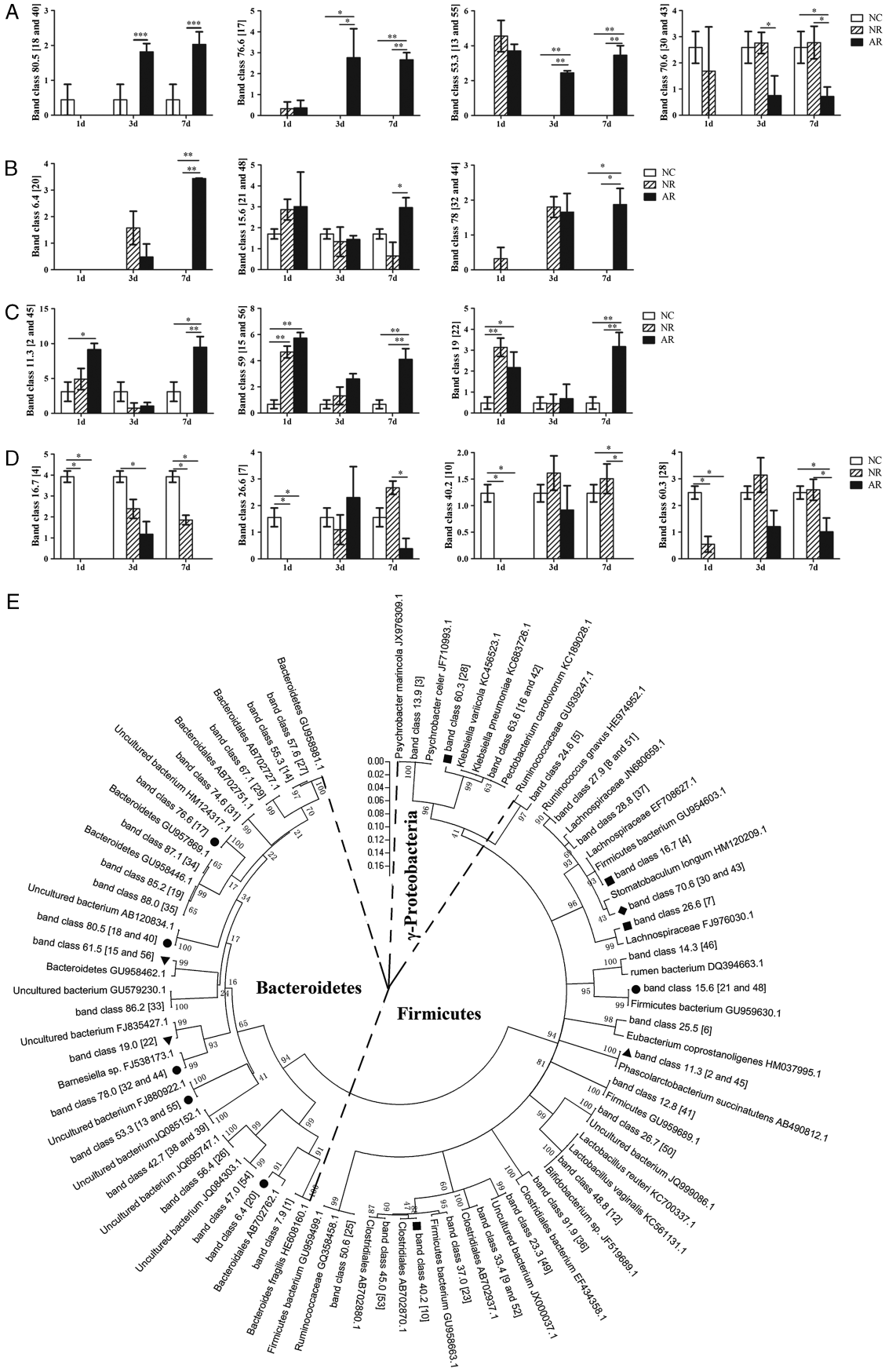
A
Band class 80.5 [18 and 40]
Band class 76.6 [17]
Band class 53.3 [13 and 55]
Band class 70.6 [30 and 43]
B
Band class 6.4 [20]
Band class 15.6 [21 and 48]
Band class 78 [32 and 44]
C
Band class 11.3 [2 and 45]
Band class 59 [15 and 56]
Band class 19 [22]
D
Band class 16.7 [4]
Band class 26.6 [7]
Band class 40.2 [10]
Band class 60.3 [28]
1d
3d
7d
NC
NR
AR
E
Bacteroidetes
Firmicutes
γ-Proteobacteria
Psychrobacter marincola JX976309.1
band class 13.9 [3]
Psychrobacter celer JF710993.1
band class 60.3 [28]
Klebsiella varricola KC456523.1
Klebsiella pneumoniae KC683726.1
band class 63.6 [16 and 42]
Pectobacterium carotovorum KC189028.1
Ruminococcaceae GU933247.1
band class 24.6 [5]
Ruminococcus gnavus HE974952.1
band class 27.9 [8 and 51]
Lachnospiraceae JN680659.1
band class 28.8 [37]
Lachnospiraceae EF708627.1
Firmicutes bacterium GU954603.1
band class 16.7 [4]
Stomatobaculum longum HM120209.1
band class 70.6 [30 and 43]
band class 26.6 [7]
Lachnospiraceae FJ976030.1
band class 14.3 [46]
rumen bacterium DQ394663.1
band class 15.6 [21 and 48]
Firmicutes bacterium GU959630.1
band class 25.5 [6]
Eubacterium coprostanoligenes HM037995.1
band class 11.3 [2 and 45]
Phascolarctobacterium succinatutens AB490812.1
band class 12.8 [41]
Firmicutes GU959689.1
band class 26.7 [50]
Uncultured bacterium JQ999086.1
Lactobacillus reuteri KC700337.1
Lactobacillus vaginalis KC561131.1
band class 48.8 [12]
Bifidobacterium sp. JF519669.1
band class 91.9 [39]
Clostridiales bacterium EF434358.1
band class 23.3 [49]
Uncultured bacterium JX000037.1
band class 33.4 [9 and 52]
Clostridiales AB702937.1
band class 37.0 [23]
Clostridiales AB702870.1
band class 40.2 [10]
Firmicutes bacterium GU958863.1
band class 45.0 [53]
Clostridiales AB702880.1
band class 50.6 [25]
Ruminococcaceae GQ358458.1
Firmicutes bacterium GU959499.1
Bacteroides fragilis HE608160.1
band class 7.9 [1]
Bacteroidales AB702762.1
band class 6.4 [20]
band class 47.0 [54]
Uncultured bacterium JQ084303.1
band class 56.4 [26]
Uncultured bacterium JQ695747.1
band class 42.7 [38 and 39]
Uncultured bacteriumJQ085152.1
band class 53.3 [13 and 55]
Uncultured bacterium FJ880922.1
band class 78.0 [32 and 44]
Barnesiella sp. FJ538173.1
band class 19.0 [22]
Uncultured bacterium FJ835427.1
band class 86.2 [33]
Uncultured bacterium GU579230.1
Bacteroidetes GU958462.1
band class 61.5 [15 and 56]
band class 80.5 [18 and 40]
Uncultured bacterium AB120834.1
band class 88.0 [35]
band class 85.2 [19]
Bacteroidetes GU958446.1
band class 87.1 [34]
Bacteroidetes GU957869.1
band class 76.6 [17]
Uncultured bacterium HM124317.1
band class 74.6 [31]
Bacteroidales AB702751.1
band class 67.1 [29]
Bacteroidales AB702727.1
band class 55.3 [14]
band class 57.6 [27]
Bacteroidetes GU959881.1
0.00
0.02
0.04
0.06
0.08
0.10
0.12
0.14
0.16

NR group, intensities of band classes 80.5 (bands 18 and 40), 76.6 (band 17), and 53.3 (bands 13 and 55) were significantly increased, whereas band class 70.6 (bands 30 and 43) was decreased in the AR group on days 3 and 7 (Fig. 4A). Meanwhile, intensities of band classes 6.4 (band 20), 15.6 (bands 21 and 48), and 78.0 (bands 32 and 44) were elevated in the AR group on day 7 (Fig. 4B). Compared with the NC group, intensities of band classes 11.3 (bands 2 and 45), 59 (bands 15 and 56), and 19 (band 22) were remarkably increased (Fig. 4C), whereas band classes 16.7 (band 4), 26.6 (band 7), 40.2 (band 10), and 60.3 (band 28) were decreased in hepatic I/R injury and severe rejection (Fig. 4D).

To clarify the phylogenetic relationship of bacterial species and find key bacteria of microbial changes during AR, the phylogenetic tree of sequences from DGGE bands was analyzed. In Figure 4(E), almost all matched bacteria of DGGE bands were allocated into three phyla: *Firmicutes* (50.0%), *Bacteroidetes* (40.9%), and *gamma-proteobacteria* (9.09%). The closest matched bacterial species corresponding to the above 14 key band classes presented in the phylogenetic tree, and the details were shown in Table S1 **SDC,** http://links.lww.com/TP/B35. In these key bacteria, all increased bacteria were assigned to phylum *Bacteroidetes* (3/3), whereas the decreased bacteria belonged to phylum *Firmicutes* in both initial and severe AR. Meanwhile, most of increased bacteria were assigned to phylum *Bacteroidetes* (2/3), whereas most of the decreased bacteria belonged to phylum *Firmicutes* (3/4) in both I/R injury and severe AR.

Dynamic Changes of Intestinal Barrier Function During AR After OLT

We observed ileal mucosal ultrastructure by transmission electron microscopy (Fig. 5A). Intestinal epithelial cells in the NC group showed a normal morphology with many homogenously distributed microvilli and integrated tight junction. On day 1, intestinal epithelial integrity in both NR and AR groups were destroyed, evidenced by microvilli loss and tight junction damage. On days 3 and 7, intestinal epithelial barrier gradually recovered near normal level in the NR group, but it first restored and then significantly damaged in the AR group, expressed by microvilli disruption, tight junction damage, and bacterial invasion.

Plasma endotoxin and tumor necrosis factor (TNF)-α were increased in the NR and AR groups versus NC group on day 1 ($P<0.01$ and $P<0.001$, respectively). On days 3 and 7, plasma endotoxin and TNF-α gradually decreased and recovered near normal level in the NR group, but they first decreased and then significantly increased in the AR group (Fig. 5B and E).

Bacterial culture in the blood was shown in Figure 5(C) and (**Table S2, SDC,** http://links.lww.com/TP/B35). The positive rates almost had no obvious differences between NR and AR groups on days 1 and 3. Notably, the positive rate was increased in the AR (6/6) versus NR groups (1/6) on day 7 ($P<0.05$).

Fecal sIgA contents were decreased in the NR and AR groups versus NC group on day 1 (both $P<0.001$). On days 3 and 7, sIgA content gradually increased and restored near normal level in the NR group, but it first increased and then remarkably decreased in the AR group (Fig. 5D).

DISCUSSION

Rejection injury is a leading cause of graft dysfunction after OLT (*5*), and few diagnostic biomarkers are clinically available for AR. An increasing studies have indicated that intestinal microbial variation is associated with various human diseases including inflammatory bowel diseases (*12*), type 2 diabetes (*21*), cardiovascular disease (*22*), liver cirrhosis (*13*), and hepatocellular carcinoma (*14, 23, 24*). Hepatic injury or disease always follows changes in intestinal permeability and microbial composition through "intestinal microbiota-liver" axis (*20*). Meanwhile, the improved hepatic graft function could promote intestinal microbial restoration (*19*), suggesting microbial profiling as a potential biomarker of liver injury. A recent study indicated that AR after OLT could induce structure shift of fecal microbiota in rats (*17*). However, so far, the dynamic relationship between AR and intestinal microbial change has not been illustrated. In this study, we established the AR model of OLT, dynamically observed rejection injury and intestinal microbial changes, and identified key microbial markers reflecting the early AR after OLT in rats.

After OLT, hepatic graft suffered from the I/R injury in both NR and AR groups on day 1, expressed by similar hepatic histology and ultrastructure as well as plasma ALT and AST. However, hepatic graft function recovered near normal level in the NR group, whereas lots of hepatocytes necrosis with inflammatory cells infiltration appeared in the AR group on day 7. Importantly, although hepatic histology and ultrastructure showed no obvious difference between both groups on day 3, plasma ALT and AST in the AR group were obviously increased, which suggested that rejection injury might initiate on day 3 and significantly aggravate on day 7.

Intestinal microbiota presented different alterations and respectively clustered together with a high similarity in hepatic I/R injury and rejection injury, which indicated that microbial profiling was helpful to distinguish liver dysfunction after OLT from hepatic I/R injury or AR. Notably, cluster

FIGURE 4. Identification of key bands of intestinal microbial changes and phylogenetic tree analysis of sequences in DGGE profiles. A, the intensities of three key bands (band classes 80.5, 76.6, and 53.3) increased and one key band (band class 70.6) decreased during the initial and severe rejection after OLT. B, the intensities of three key bands (band classes 6.4, 15.6, and 78) increased during only severe rejection after OLT. C, the intensities of three key bands (band classes 11.3, 59, and 19) increased and (D) four key bands (band classes 16.7, 26.6, 40.2, and 60.3) decreased during the I/R injury and severe rejection after OLT. E, phylogenetic tree analysis of sequences from DGGE profiles using the neighbor-joining method. Twenty-eight band classes without labels showed little variation among the different groups. Six band classes labeled with black spot showed an increase and one band class labeled with black diamond showed a decrease during only rejection. Three band classes labeled with black triangle showed an increase and four band classes labeled with black square showed a decrease during the I/R injury and rejection after OLT. The plot was obtained from MEGA5 software (http://en.wikipedia.org/wiki/MEGA,_Molecular_Evolutionary_Genetics_Analysis). OLT, orthotopic liver transplantation; I/R, ischemia-reperfusion.

analysis showed that the 7AR and 3AR groups clustered together with 73.4% similarity, suggesting a high similarity in microbial composition between day 3 and day 7 after OLT in the AR group. However, graft structure had no significant aggravation on day 3, whereas the obvious hepatic rejection appeared on day 7. These data suggested that intestinal microbiota was more sensitive than hepatic histology in responding to hepatic rejection injury after OLT. Thus, we hypothesized that intestinal microbial shift on day 3 after OLT could predict AR in early phase before severe aggravation of graft function. Next, we found four key bands of microbial shift in both the early and severe AR injuries. These key bacteria may become an auxiliary diagnosis marker for the early AR after OLT.

The "microbiota-liver" axis closely links intestinal microbiota and liver function in health and disease (*20*). Intestinal microbiota is a complex ecological structure with an extensive microbial population (*6, 9*), thus how acute rejection causes microbial changes is an important question. On one hand, AR after OLT may induce partial graft dysfunction and transient portal hypertension (*25*), which may lead to intestinal microcirculation disturbance including intestinal I/R injury (*26*), thereby inducing alterations in intestinal permeability and microbial composition (*27*). Similar mechanism may also happen in cirrhotic patients. In patients with liver cirrhosis, fecal microbiota changes mainly presented the prevalence of potentially pathogenic bacteria, such as *Enterobacteriaceae* and *Streptococcaceae*, with the reduction of beneficial populations, such as *Lachnospiraceae* (*13*). On the other hand, inflammation induced by AR plays a central role in microbial alterations. Intestinal mucosal immune system can detect and clear most food-borne pathogens, and keep potential opportunists in check without excess harm to host tissues through Toll-like receptor (TLR) and nucleotide-binding oligomerization domain-like (NLR) receptor recognizing various bacterial products including lipopolysaccharide and bacterial DNA (*20*). Acute rejection after OLT can trigger cascade reaction of substantial proinflammatory factors production and release to activate TLR-NLR pathways (*28*), thereby initiating intestinal mucosal immune system to clear the bacteria. For example, small bowel transplantation rejection was associated with alterations in microbial populations in ileal effluents (*16*). In contrast, during AR, altered microbial composition can result in microbial products activating TLR and NLR of the innate immune system, thereby driving proinflammatory gene expression that aggravates liver rejection injury (*20*). Thus, intestinal microbial profiling may become a potential biomarker predicting liver injury or rejection after OLT.

Intestinal barrier dysfunction or various intestinal diseases such as irritable bowel syndrome (*29*), Crohn's disease (*30, 31*), and inflammatory bowel diseases (*32*) always accompany alterations of microbial composition, but the causal relationship between intestinal barrier dysfunction and microbial variation remains unclear. Thus, we further tested intestinal barrier function including epithelial integrity, endotoxin, TNF-α, and fecal sIgA, and found intestinal barrier damage from hepatic I/R injury on day 1, partial restoration on day 3, and significant aggravation on day 7 after OLT. However, cluster analysis showed that the 7AR and 3AR groups clustered together with 73.4% similarity, which suggested that intestinal microbial variation preceded barrier dysfunction. These results may hint that alterations of intestinal barrier function from day 3 to day 7 were partly attributed to microbial disruption during hepatic rejection injury.

There has been growing interest in the therapeutic potential of fecal microbiota transplantation for chronic gastrointestinal infections (*33*), inflammatory bowel diseases (*34*), cardiovascular diseases (*22*), metabolic diseases, and autoimmune diseases (*35*). In a recent randomized controlled trial, duodenal infusion of donor feces was significantly more effective for the treatment of recurrent *Clostridium difficile* infection than the use of vancomycin (*36*). Thus, intestinal microbiota can be manipulated to become a safe and promising treatment of human diseases. Because of "microbiota-liver" axis, liver diseases can lead to intestinal microbial disruption, and microbial imbalance can aggravate liver disease (*14, 20*), which also happens in hepatic AR after OLT. Therefore, intestinal microbial variation may become an assistant therapeutic target to stop the vicious circle of "microbiota-liver" axis, thereby improving hepatic rejection injury after OLT.

In conclusion, hepatic rejection injury after OLT can induce intestinal microbial alteration in early phase and subsequent intestinal barrier dysfunction, which may in turn aggravate hepatic rejection injury in the late phase. Because of a high sensitivity of microbial change during AR after OLT, intestinal microbial variation may predict AR in early phase after OLT, and also become an assistant therapeutic target to improve rejection injury after OLT.

MATERIALS AND METHODS

Animals

Specific pathogen-free Lewis rats were purchased from Beijing Vital River Laboratories; specific pathogen-free DA rats were purchased from Animal Resources Centre, Murdoch, Western Australia and breed in the laminar flow cabinet. All rats were housed in Laboratory Animals Center of First Affiliated Hospital, School of Medicine, Zhejiang University. The rats were caged in 21°C, 12 hr light-dark cycle, and fed with sterilized standard rat chow and water.

Experimental Protocol

The rats (weight 220–250 g) after OLT were divided into two groups. (i) The NR group (n=18): both donors and recipients were Lewis rats. (ii) The AR group (n=18): donors were DA and recipients were Lewis rats. Rats were sacrificed by overdose anesthesia and sampled at days 1, 3, and 7 after OLT, respectively (n=6). Meanwhile, six healthy Lewis rats were sampled as NC group. All procedures were performed according to "Guide for the Care and Use of Laboratory Animals" published by the National Institutes of Health (publication 86-23 revised 1985). The protocols were approved by Animal Care and Use Committee of First Affiliated Hospital, School of Medicine, Zhejiang University.

Surgical Procedures, Sample Collection, and Tests

The OLT models, sample collection, and testing methods of liver histology and function, liver and intestine ultrastructure, DNA extraction of ileocecal content, and intestinal barrier function test were established according to our previous techniques (*19, 37–39*).

Real-Time qPCR

Real-time qPCR was performed using a DNA Engine Opticon 2 apparatus (Bio-Rad, Hercules, CA) with the Opticon Monitor software (version 3.0; Bio-Rad), as our previous operations (*19*). The primers for the genetic determinants and annealing temperatures were shown in Table S3 (**SDC,** http://links.lww.com/TP/B35).

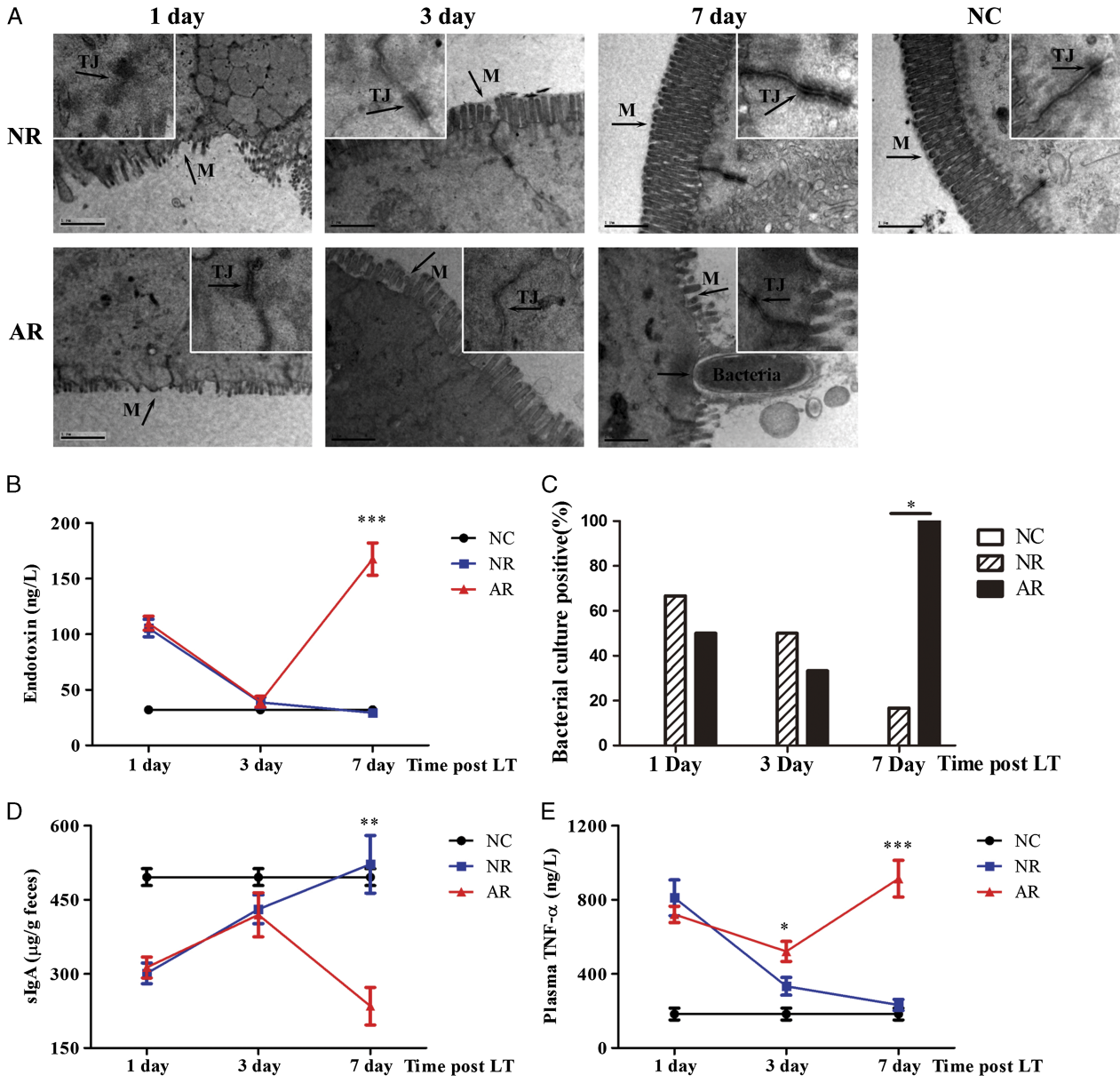

FIGURE 5. Dynamic changes of intestinal barrier function during AR after OLT. A, representative intestinal mucosal ultrastructure observed by TEM between the NR and AR groups at different time points after OLT. B, changes of plasma endotoxin were observed among the different groups. C, the positive rates of bacterial culture in the blood were shown in the different groups. D, fecal sIgA content was calculated by ELISA and expressed as micrograms (μg) per gram wet feces in the different groups. E, plasma level of TNF-α was detected by ELISA in the different groups. *P<0.05, **P<0.01, ***P<0.001. TEM, transmission electron microscopy; AR, acute rejection; OLT, orthotopic liver transplantation; TNF, tumor necrosis factor; ELISA, enzyme-linked immunosorbent assay; M, microvilli; TJ, tight junction; NR, nonrejection, AR, acute rejection.

DGGE Profiling

DGGE was performed using the D-Code universal mutation detection system apparatus (Bio-Rad). DGGE profiles were processed digitally using BioNumerics software version 6.01 (Applied Maths, St-Martens-Latem, Belgium) (*19*). Cluster analysis of DGGE profiles were performed with the unweighted pair-group method.

Sequencing of DGGE Bands

The interested DGGE bands were excised and sequenced. The detailed sequencing process of DGGE bands referred to our previous study (*19*). The phylogenetic tree was constructed using MEGA 5.0 program by the neighbor-joining method based on evolutionary distances.

Statistical Analysis

All data are expressed as mean±standard error of the mean. For parametric data, statistical significance among groups was compared by one-way analysis of variance analysis. For nonparametric data, Kruskal-Wallis followed by Dunn's multiple comparison tests was used. Statistical analyses were conducted using SPSS version 17.0 for Windows (SPSS Inc., Chicago, IL).

ACKNOWLEDGMENTS

The authors thank Prof. Jimin Liu (Department of Pathology and Molecular Medicine, Faculty of Health Sciences, McMaster University, Hamilton, ON, Canada) for critically reading the article.

REFERENCES

1. Hubscher SG. What is the long-term outcome of the liver allograft? *J Hepatol* 2011; 55: 702.
2. Sayegh MH, Carpenter CB. Transplantation 50 years later—progress, challenges, and promises. *N Engl J Med* 2004; 351: 2761.
3. Kim WR, Stock PG, Smith JM, et al. OPTN/SRTR 2011 annual data report: liver. *Am J Transplant* 2013; 13(Suppl 1): 73.
4. Kim WR, Smith JM, Skeans MA, et al. OPTN/SRTR 2012 annual data report: liver. *Am J Transplant* 2014; 14(Suppl 1): 69.
5. Hu J, Wang Z, Tan CJ, et al. Plasma microRNA, a potential biomarker for acute rejection after liver transplantation. *Transplantation* 2013; 95: 991.
6. Eckburg PB, Bik EM, Bernstein CN, et al. Diversity of the human intestinal microbial flora. *Science* 2005; 308: 1635.
7. Nenci A, Becker C, Wullaert A, et al. Epithelial NEMO links innate immunity to chronic intestinal inflammation. *Nature* 2007; 446: 557.
8. Cani PD, Delzenne NM. The role of the gut microbiota in energy metabolism and metabolic disease. *Curr Pharm Des* 2009; 15: 1546.
9. Gill SR, Pop M, Deboy RT, et al. Metagenomic analysis of the human distal gut microbiome. *Science* 2006; 312: 1355–9.
10. Ley RE, Peterson DA, Gordon JI. Ecological and evolutionary forces shaping microbial diversity in the human intestine. *Cell* 2006; 124: 837.
11. Backhed F, Ley RE, Sonnenburg JL, et al. Host-bacterial mutualism in the human intestine. *Science* 2005; 307: 1915.
12. Sartor RB. Microbial influences in inflammatory bowel diseases. *Gastroenterology* 2008; 134: 577.
13. Chen Y, Yang F, Lu H, et al. Characterization of fecal microbial communities in patients with liver cirrhosis. *Hepatology* 2011; 54: 562.
14. Dapito DH, Mencin A, Gwak GY, et al. Promotion of hepatocellular carcinoma by the intestinal microbiota and TLR4. *Cancer Cell* 2012; 21: 504.
15. Li Q, Zhang Q, Wang C, et al. Fish oil enhances recovery of intestinal microbiota and epithelial integrity in chronic rejection of intestinal transplant. *PLoS One* 2011; 6: e20460.
16. Oh PL, Martinez I, Sun Y, et al. Characterization of the ileal microbiota in rejecting and nonrejecting recipients of small bowel transplants. *Am J Transplant* 2012; 12: 753.
17. Xie Y, Luo Z, Li Z, et al. Structural shifts of fecal microbial communities in rats with acute rejection after liver transplantation. *Microb Ecol* 2012; 64: 546.
18. Xing HC, Li LJ, Xu KJ, et al. Protective role of supplement with foreign Bifidobacterium and Lactobacillus in experimental hepatic ischemia-reperfusion injury. *J Gastroenterol Hepatol* 2006; 21: 647.
19. Ren Z, Cui G, Lu H, et al. Liver ischemic preconditioning (IPC) improves intestinal microbiota following liver transplantation in rats through 16 s rDNA-based analysis of microbial structure shift. *PLoS One* 2013; 8: e75950.
20. Chassaing B, Etienne-Mesmin L, Gewirtz AT. Microbiota-liver axis in hepatic disease. *Hepatology* 2014; 59: 328.
21. Qin J, Li Y, Cai Z, et al. A metagenome-wide association study of gut microbiota in type 2 diabetes. *Nature* 2012; 490: 55.
22. Wang Z, Klipfell E, Bennett BJ, et al. Gut flora metabolism of phosphatidylcholine promotes cardiovascular disease. *Nature* 2011; 472: 57.
23. Darnaud M, Faivre J, Moniaux N. Targeting gut flora to prevent progression of hepatocellular carcinoma. *J Hepatol* 2013; 58: 385.
24. Zhang HL, Yu LX, Yang W, et al. Profound impact of gut homeostasis on chemically-induced pro-tumorigenic inflammation and hepatocarcinogenesis in rats. *J Hepatol* 2012; 57: 803.
25. Bedi DS, Riella LV, Tullius SG, et al. Animal models of chronic allograft injury: contributions and limitations to understanding the mechanism of long-term graft dysfunction. *Transplantation* 2010; 90: 935.
26. Maksan SM, Ryschich E, Ulger Z, et al. Disturbance of hepatic and intestinal microcirculation in experimental liver cirrhosis. *World J Gastroenterol* 2005; 11: 846.
27. Wang F, Li Q, Wang C, et al. Dynamic alteration of the colonic microbiota in intestinal ischemia-reperfusion injury. *PLoS One* 2012; 7: e42027.
28. Mori DN, Kreisel D, Fullerton JN, et al. Inflammatory triggers of acute rejection of organ allografts. *Immunol Rev* 2014; 258: 132.
29. Jalanka-Tuovinen J, Salojarvi J, Salonen A, et al. Faecal microbiota composition and host-microbe cross-talk following gastroenteritis and in postinfectious irritable bowel syndrome. *Gut* 2013; 0: 1.
30. Baumgart DC, Sandborn WJ. Crohn's disease. *Lancet* 2012; 380: 1590.
31. Joossens M, Huys G, Cnockaert M, et al. Dysbiosis of the faecal microbiota in patients with Crohn's disease and their unaffected relatives. *Gut* 2011; 60: 631.
32. Chassaing B, Darfeuille-Michaud A. The commensal microbiota and enteropathogens in the pathogenesis of inflammatory bowel diseases. *Gastroenterology* 2011; 140: 1720.
33. Surawicz CM, Brandt LJ, Binion DG, et al. Guidelines for diagnosis, treatment, and prevention of *Clostridium difficile* infections. *Am J Gastroenterol.* 2013; 108: 478 quiz 99.
34. Jeffery IB, O'Toole PW, Ohman L, et al. An irritable bowel syndrome subtype defined by species-specific alterations in faecal microbiota. *Gut* 2012; 61: 997.
35. Smits LP, Bouter KE, de Vos WM, et al. Therapeutic potential of fecal microbiota transplantation. *Gastroenterology* 2013; 145: 946.
36. van Nood E, Vrieze A, Nieuwdorp M, et al. Duodenal infusion of donor feces for recurrent *Clostridium difficile. N Engl J Med* 2013; 368: 407.
37. Ren ZG, Liu H, Jiang JW, et al. Protective effect of probiotics on intestinal barrier function in malnourished rats after liver transplantation. *Hepatobiliary Pancreat Dis Int* 2011; 10: 489.
38. Ren Z, Chen X, Cui G, et al. Nanosecond pulsed electric field inhibits cancer growth followed by alteration in expressions of NF-kappaB and Wnt/beta-catenin signaling molecules. *PLoS One* 2013; 8: e74322.
39. Lu H, He J, Wu Z, et al. Assessment of microbiome variation during the perioperative period in liver transplant patients: a retrospective analysis. *Microb Ecol* 2013; 65: 781.